TRENDS IN SCIENCES 2025; 22(8): 10189
https://doi.org/10.48048/tis.2025.10189 RESEARCH ARTICLE

The Synthesis of Activated Carbon from Agricultural Residues for Application as an Adsorbent Via Easy Method and Using the Innovative Simple Biomass Incinerator

Tappagorn Leelatam[1,2,3], Wuttichai Roschat[2,3,4,*], Thanaphon Fongwichai[2,4], Warisara Tamprasee[2,4], Sunti Phewphong[2,3], Preecha Moonsin[5], Prawit Nuengmatcha[6], Prawit Suwannarong[7] and Vinich Promarak[8]

[1]*Appropriated Technology Center, Faculty of Science and Technology, Sakon Nakhon Rajabhat University, Sakon Nakhon 47000, Thailand*
[2]*Biomass Energy Research Laboratory, Center of Excellence on Alternative Energy, Research and Development Institution, Sakon Nakhon Rajabhat University, Sakon Nakhon 47000, Thailand*
[3]*Innovation in Chemistry for Community Research Unit, Faculty of Science and Technology, Sakon Nakhon Rajabhat University, Sakon Nakhon 47000, Thailand*
[4]*Program of Chemistry, Faculty of Science and Technology, Sakon Nakhon Rajabhat University, Sakon Nakhon 47000, Thailand*
[5]*Program of Chemistry, Faculty of Science, Ubon Ratchathani Rajabhat University, Ubon Ratchathani 34000, Thailand*
[6]*Center of Excellence in Nanomaterials Chemistry, Faculty of Science and Technology, Nakhon Si Thammarat Rajabhat University, Nakhon Si Thammarat 80280, Thailand*
[7]*Program of Environment Science, Faculty of Science and Technology, Sakon Nakhon Rajabhat University, Sakon Nakhon 47000, Thailand*
[8]*Department of Material Science and Engineering, School of Molecular Science & Engineering, Vidyasirimedhi Institute of Science and Technology, Rayong 21210, Thailand*

(*Corresponding author's e-mail: roschat1@gmail.com)

Received: 17 March 2025, Revised: 20 April 2025, Accepted: 20 April 2025, Published: 25 June 2025

Abstract

Activated carbon is widely used in environmental and industrial applications due to its high adsorption capacity. This research aimed to utilize agricultural waste materials—rubber wood twigs, rubber seed pods, *Leucaena leucocephala* wood, and coconut shells—as precursors for the production of activated carbon, addressing the increasing need for low-cost and sustainable adsorbents. Both dry and wet chemical activation methods were employed using sodium hydroxide (NaOH) in conjunction with a biomass incinerator. Among all the samples, activated carbon derived from rubber wood twigs (AC/rwt) via dry activation demonstrated the most favorable properties. Comprehensive characterization was conducted using X-ray diffraction (XRD), Brunauer–Emmett–Teller (BET) surface area analysis, transmission electron microscopy (TEM), energy-dispersive X-ray spectroscopy (EDS), scanning electron microscopy (SEM), and Fourier-transform infrared spectroscopy (FT-IR). Adsorption efficiency was evaluated through iodine number measurement and methylene blue adsorption tests. The AC/rwt sample exhibited a specific surface area of 726.60 m^2/g, an iodine number of 616.73 mg/g, and a methylene blue adsorption efficiency of 99.65 %, which complies with Thailand's industrial standard TIS 900 - 2004. Elemental analysis confirmed that carbon was the predominant element in all samples. Additionally, the pore size distribution indicated mesoporous structures ranging from 2 - 50 nm. Although commercial activated carbon outperformed in some metrics (950.02 m^2/g surface area, 743.77 mg/g iodine number, and 100 % methylene blue adsorption), this study demonstrates that agricultural waste can be successfully converted into high-quality activated carbon suitable for diverse adsorbent applications.

Keywords: Activated carbon, Rubberwood twigs, Adsorbent, Iodine adsorption value, Innovative simple biomass incinerator

Introduction

Activated carbon is a form of carbonaceous material that has been processed to develop a highly porous structure, significantly increasing its surface area and adsorption capacity. Unlike normal charcoal, which is primarily used as a fuel and has limited porosity, activated carbon undergoes either physical or chemical activation processes that result in an extensive network of micro-, meso-, and macropores. These structural differences give activated carbon superior adsorption properties, making it highly effective in capturing a wide range of contaminants. Activated carbon is valued for its high surface area, typically ranging from 600 to 2400 m^2/g, and pore volume between 0.20 and 1.00 cm^3/g, which are critical factors influencing its performance [1-5]. One of the most important indicators of activated carbon quality is its iodine number, which reflects its capacity to adsorb small molecular weight compounds. According to Thailand Industrial Standard (TIS 900 - 2004), the iodine number must not be less than 600 mg/g for the material to be classified as activated carbon [1,4]. Other relevant properties include pore size distribution, adsorption of inert gases (e.g., nitrogen in BET analysis), and mechanical strength, which together determine its effectiveness and durability in practical applications. Activated carbon is widely used across various industries due to its excellent adsorption efficiency. Common applications include water and air purification, food and beverage processing, pharmaceuticals, petrochemicals, chemical manufacturing, sugar refining, and dye removal. In powdered form, it is often incorporated into water filters and decolorizing agents [6-13]. A diverse range of raw materials can be used for its production, including wood, coconut shells, coal, and various types of agricultural biomass waste. The selection of raw material, along with the activation method, greatly influences the physicochemical characteristics and final performance of the activated carbon.

The production of activated carbon involves 2 primary methods: Physical and chemical activation. Chemical activation is preferred due to its simpler process, shorter preparation time, and lower activation temperatures. It results in activated carbon with higher surface area, larger pore volume, and better adsorption efficiency. Common chemicals used as activating agents include KOH, NaOH, K_2CO_3, Na_2CO_3, HCl, KCl, $AgCl_3$, and $ZnCl_2$, with KOH and NaOH being the most cost-effective and accessible [4,9,10,13-16]. In a work by Mistar *et al.* [10], a 2-step KOH activation procedure was used to create activated carbon from *Bambusa vulgaris* Schrad. A 1:3 char to KOH ratio, an activation duration of 1 h, and an activation temperature of 800 °C were determined to be the optimal parameters. This produced a BET surface area of 980 m^2/g and a pore volume of 0.559 cm^2/g. SEM and FT-IR analyses confirmed high porosity and the presence of various functional groups. Cazetta *et al.* [17] prepared activated carbon from coconut shells using NaOH activation at different impregnation ratios (1:1, 2:1, 3:1). The resulting activated carbons were predominantly microporous, with BET surface areas of of 783, 1842, and 2825 m^2/g for AC-1, AC-2, and AC-3, respectively. Sarawanan *et al.* [18] used activated carbon from oil palm empty fruit bunches that had been prewashed in NaOH to optimize a 2-stage adsorber for the removal of methylene blue. The adsorbent mass was lowered by 6.67 % using this approach, and the equilibrium time was notably shortened from 22 to 0.52 h. Because stage 1's larger adsorbent mass reduced the effort required to reach equilibrium, industrial dye removal became economically viable.

Using NaOH activation, Yahya *et al.* [19] examined the impact of temperature and impregnation ratio on the characteristics of activated carbon derived from desiccated coconut residue (DCR). DCR was carbonized for 1 h at 400, 500, and 600 °C. After that, the chars were impregnated with NaOH in ratios of 1:1, 2:2, and 1:3, and they were activated for 1 h at the appropriate carbonization temperatures under nitrogen. According to the research, the specific surface area rose at higher impregnation ratios and temperatures up to 500 °C but fell at 600 °C. By using a 1:3 ratio and activation temperature of 500 °C, the maximum BET surface area of around 1394.79 m^2/g was attained. Using batch and fixed-bed methods, Khan *et al.* [20] investigated the adsorption of methyl orange and malachite green onto waste tire activated carbon. Using KOH as the activating agent at 700 °C for 2 h and a pH of 7, the resulting activated carbon had a surface area of 490 m^2/g. Lv *et*

al. [21] synthesized activated carbon for phenol adsorption by pyrolyzing rice husk, followed by KOH activation and EDTA-4Na modification. Carbonized at 500 °C and activated at 750 °C with a carbon to KOH ratio of 1:3, the activated carbon exhibited rich microporosity, a high specific surface area of 2087 m^2/g, and a maximum phenol adsorption capacity of 194.24 mg/g.

Despite the extensive research on activated carbon derived from various biomass sources—such as Bambusa vulgaris Schrad., coconut shells, oil palm empty fruit bunches, desiccated coconut residue, rice husks, and even waste tires—there remains a critical gap in the utilization of locally abundant and underutilized agricultural residues. Many existing methods require high temperatures, multi-step procedures, or costly chemical modifications, which may limit their practical application, especially in rural areas. Furthermore, few studies have systematically compared different types of agricultural waste using a consistent activation method that is accessible, energy-efficient, and suitable for community-level implementation. Therefore, this research aims to address this gap by synthesizing activated carbon from agricultural residues specific to Sakon Nakhon Province, Thailand, including rubber wood twigs, rubber seed pods, *Leucaena leucocephala* wood, and coconut shells. These materials are locally available yet often discarded as waste, representing an untapped resource for value-added applications. An inventive biomass incinerator developed by the Appropriate Technology Center of Sakon Nakhon Rajabhat University was employed for the carbonization process. This prototype incinerator was specifically designed for efficient carbonization of agricultural biomass and featured a controlled air-flow system, high thermal insulation, and uniform heat distribution. Its design allowed for consistent temperatures necessary for producing high-quality charcoal while minimizing incomplete combustion and emissions, as shown in the details of its components and working principle in **Figure 1** [13,14]. The choice of this incinerator is based on its suitability for small-scale, community-based applications and its ability to convert various types of agricultural waste—such as rubber wood twigs, rubber seed pods, *Leucaena leucocephala* wood, and coconut shells—into carbonized material with enhanced yield and quality. These features make it particularly well-aligned with the goals of this study, which seeks to transform local biomass waste into value-added activated carbon.

The study focused on comparing dry and wet chemical activation methods using NaOH, with an emphasis on dry activation due to its simplicity and energy efficiency, as illustrated in **Figure 1**. The resulting activated carbon was characterized using XRD, FT-IR, SEM, TEM, EDS, and BET surface area analysis. Adsorption performance was assessed through iodine number measurement and methylene blue adsorption tests. The central hypothesis was that these agricultural residues could be converted into activated carbon with physicochemical properties that meet or exceed the industrial standard TIS 900 - 2004 set by the Ministry of Industry of Thailand. Ultimately, the study aimed to generate practical data and recommendations to empower local communities with the capability to produce cost-effective, high-quality activated carbon for environmental and industrial applications.

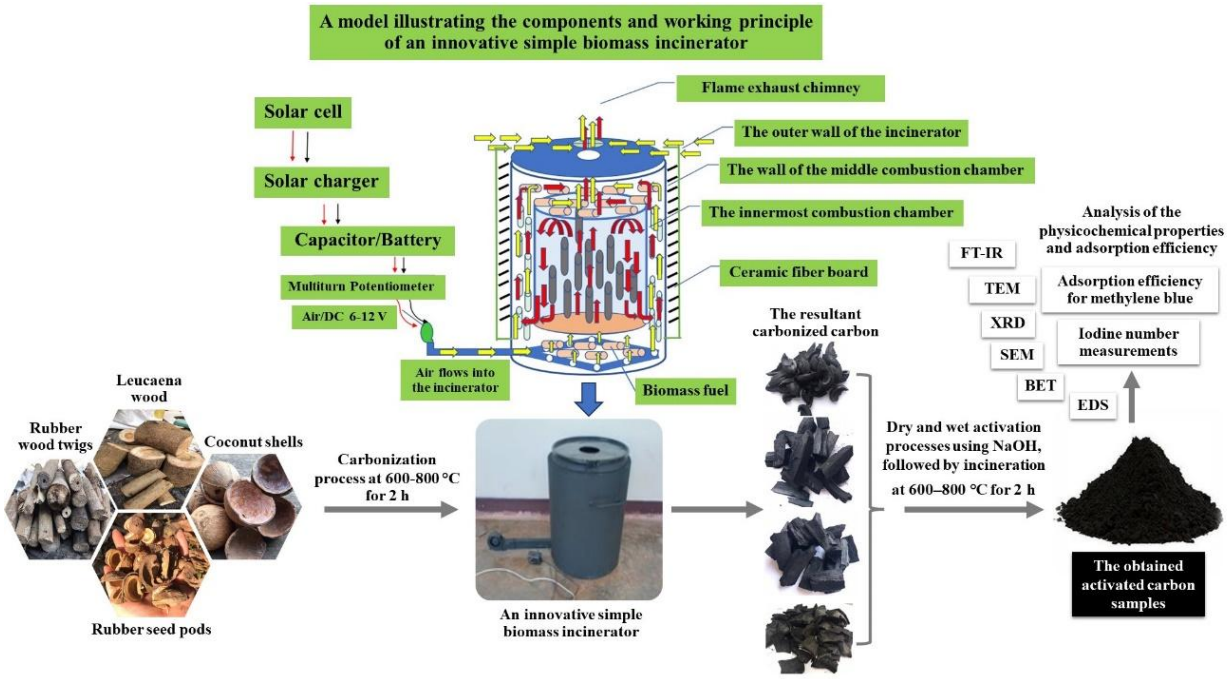

Figure 1 A model illustrating the components and working principle of an innovative simple biomass incinerator, along with the flow diagram for synthesizing activated carbon from agricultural residues.

Materials and methods

Materials

This research collected samples of agricultural waste materials in Sakon Nakhon province, Thailand, consisting of 4 types namely coconut shells, rubber wood twigs, rubber seed pods, and Leucaena wood. All samples of raw material were crushed into small pieces of about 3 to 5 cm. The chemicals used for this experimental study included NaOH, HCl, $Na_2S_2O_3$, I_2 pellets, KIO_3, and Na_2CO_3, all of which were AR grade and purchased from Qrëc (Newzealand). Meanwhile, KI of LAB grade was purchased from Ajax Finechem (Australia), and methylene blue of LAB grade was from the KemAus^{TM} brand (Australia).

Preparation of carbonized carbon from agricultural waste materials

Agricultural waste materials prepared into small pieces were packed into containers and weighed before incineration. Afterward, they were burned in a carbonization process at temperatures between 600 - 800 °C for 2 h using an innovative simple biomass incinerator. The resultant carbonized carbon was left to cool before being weighed. Subsequently, a portion of the produced charcoal was finely ground and sifted through a 60-mesh sieve (approximately 0.25 mm) to prepare samples for analysis. As depicted in **Figure 2**, the process diagram shows the preparation of carbonized carbon and activated carbon from agricultural waste materials. Each type of carbonized carbon was labeled with an abbreviation representing the agricultural waste material it originated from: CP/rwt for rubber wood twigs, CP/rsp for rubber seed pods, CP/Lw for Leucaena wood, and CP/cs for coconut shells.

Activated carbon preparation

This research investigated the synthesis of activated carbon using 2 activation methods namely dry activation and wet activation as illustrated in **Figure 2**. The following abbreviation symbols will be used throughout the study: C/AC for commercial activated carbon which used as a comparison with synthetic activated carbon; AC/rwt for activated carbon obtained from rubber wood twigs; AC/rsp for activated carbon obtained from rubber seed pods; AC/Lw for activated carbon obtained from Leucaena wood; and AC/cs for

activated carbon obtained from coconut shells, respectively.

Study of dry activation methods

The activation of raw charcoal was carried out using a dry chemical method with NaOH as the activating agent. Ground charcoal powder (100 g), obtained from the carbonization of agricultural residues, was mixed with 300 g of solid NaOH, maintaining a weight ratio of 1:3 (char:NaOH). The mixture was then incinerated at a temperature range of 600 - 800 °C for 2 h using an innovative biomass incinerator developed by the Appropriate Technology Center at Sakon Nakhon Rajabhat University. After incineration, the product was allowed to cool to room temperature. Subsequently, the resulting activated carbon was washed with distilled water by boiling at approximately 80 °C for 30 min to remove residual chemicals. The mixture was filtered using a vacuum filtration system and rinsed repeatedly with distilled water until the filtrate reached a neutral pH (pH = 7). The washed activated carbon was then dried in a hot air oven at 110 °C overnight. Finally, the dried samples were ground thoroughly and stored in sealed, zippered sample bags in preparation for further characterization and analysis. This procedure constituted a 2-step dry activation process.

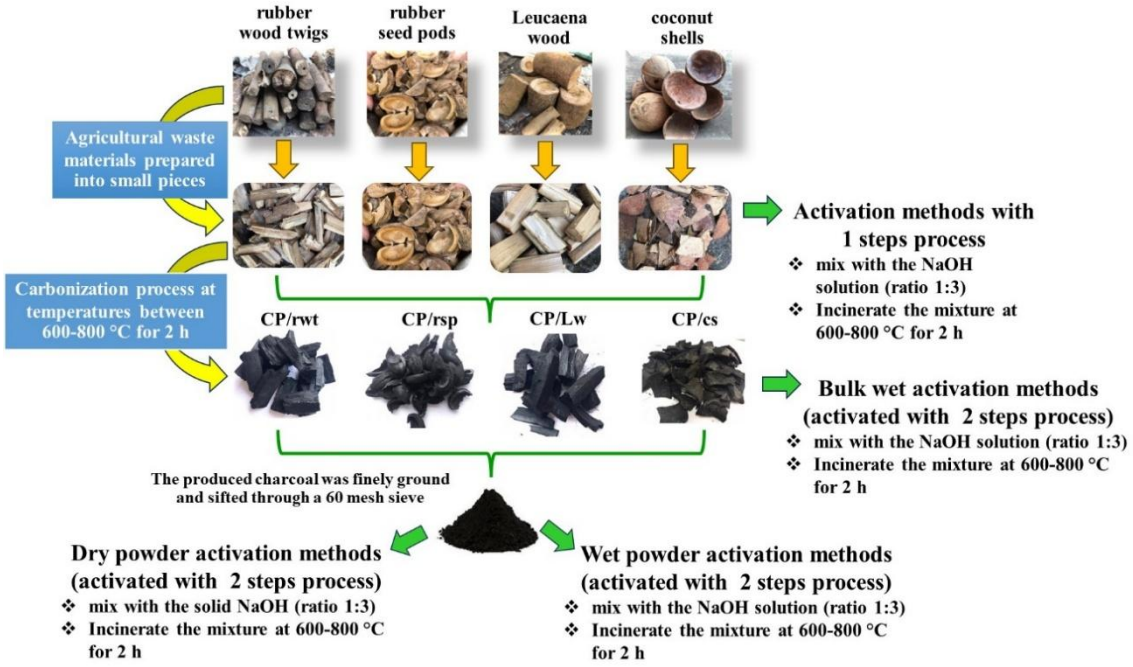

Figure 2 The process diagram depicts the preparation of carbonized carbon and activated carbon from agricultural waste materials.

Study of wet activation methods

This study investigated the wet activation method for producing activated carbon, which was divided into 3 distinct experimental approaches based on the form and pre-treatment of the raw materials. These included: (1) activation of powdered charcoal derived from carbonized biomass, (2) activation of non-powdered (bulk) charcoal derived from carbonized biomass, and (3) direct activation of raw wood that had not undergone carbonization.

In the first method, 100 g of charcoal powder obtained from the carbonization process were soaked in 300 g of NaOH solution, prepared by dissolving the NaOH in 1 L of distilled water. The mixture was left to soak for 24 h. Afterward, the slurry was filtered using a vacuum filtration system. The solid residue was then subjected to thermal activation by incineration at 600 - 800 °C for 2 h using an innovative simple biomass incinerator. The activated carbon was left to cool, then rinsed repeatedly with distilled water until a neutral pH

(pH = 7) was achieved. It was subsequently dried at 110 °C for 12 h, finely ground, and stored in a sealed zipper bag for further analysis. This method is referred to as the wet powder 2-step activation process.

The second method followed a similar procedure but used non-powdered, bulk charcoal obtained from carbonized biomass. In this case, 100 g of the bulk charcoal were soaked in 300 g of NaOH solution (in 1 L of distilled water) for 24 h. The charcoal was then filtered, incinerated at 600 - 800 °C for 2 h, and allowed to cool. It was then roughly ground and washed with distilled water until neutral pH was achieved. The product was dried at 110 °C for 12 h, finely ground, sieved through a 60-mesh (approximately 0.25 mm) sieve, and stored in a zipper bag for subsequent property evaluation. This is defined as a wet bulk 2-step activation process.

In the third method, raw wood that had not undergone carbonization was directly activated. Here, 100 g of raw wood were soaked in 300 g of NaOH solution (dissolved in 1 L of distilled water), followed by filtration. The impregnated wood was then incinerated at 600 - 800 °C for 2 h, cooled, and roughly ground. The resulting material was washed with distilled water until reaching neutral pH, dried at 110 °C for 12 h, finely ground, sieved through a 60-mesh screen, and stored in a zipper bag for further analysis. This is categorized as a 1-step activation process since carbonization and chemical activation occur simultaneously during the high-temperature treatment.

By comparing these 3 methods, the study aimed to determine how the physical state and preparation of the raw materials influence the properties of the resulting activated carbon, ultimately guiding the selection of an efficient and practical production method for community or industrial applications.

Analysis of the physicochemical properties and adsorption efficiency of the obtained activated carbon samples

The activated carbon samples derived from agricultural waste and prepared by various methods were thoroughly characterized using multiple analytical techniques. X-ray diffraction (XRD) analysis was conducted using an X'Pert Pro MPD model manufactured by PANalytical (Malvern Panalytical), Netherlands; however, the analysis itself was performed locally in Thailand. The XRD was operated under the following conditions: Cu Kα radiation (λ = 1.5406 Å), operating voltage of 40 kV, current of 30 mA, and a scanning range of 20 to 80 ° (2θ) at a step size of 0.02 °. Surface area and porosity analyses were carried out using the BET-sorp mini II, manufactured by BEL, Japan, with nitrogen adsorption-desorption at 77 K. The specific surface area was calculated using the BET method, and pore volume and size distribution were determined using the Barrett-Joyner-Halenda (BJH) method. Transmission Electron Microscopy with Energy Dispersive X-ray Spectroscopy (TEM-EDS) was performed using a TECNAI G2 20 model by FEI, Netherlands, operated at an accelerating voltage of 200 kV, to examine the internal morphology and elemental composition of the activated carbon.

Scanning Electron Microscopy (SEM) was conducted using a QUANTA 450 model by FEI, France, at an accelerating voltage of 10 kV under high vacuum conditions to observe surface morphology at a magnification of 500-fold. The analysis was performed in Back Scattered Electron (BSE) mode to enhance contrast and provide detailed information on the composition and structure of the samples. Fourier Transform Infrared (FT-IR) spectroscopy analysis was performed using a SHIMADZU FT-IR-8900, made in Japan, with a spectral range of 500 - 4000 cm^{-1} with a resolution of 4 cm^{-1} and 32 scans per sample. To evaluate adsorption efficiency, iodine number determination was carried out according to TIS 900 - 2004, as established by the Ministry of Industry of Thailand [1,4,13], and methylene blue adsorption capacity was measured using methods adapted from Pathania *et al.* [22]. The efficiency of dye adsorption was reported in terms of the percentage removal of methylene blue, calculated by the difference between the initial concentration of methylene blue and the residual concentration of methylene blue. The calculated difference was then divided by the initial concentration of methylene blue and expressed as the percentage of methylene blue removal. The final methylene blue concentration was determined by spectrophotometry at 665 nm wavelength using the calibration curve. All adsorption experiments were performed in triplicate, and results were reported as mean values with deviations within ± 3 %.

Results and discussion

The physicochemical adsorption efficiency analysis

The analysis of iodine adsorption values

This research investigated the physicochemical adsorption efficiency of activated carbon samples in comparison to raw charcoal and commercial activated carbon. The study analyzed the iodine adsorption value according to the TIS 900-2004 standard of Thailand, which is reported as the amount of iodine adsorbed (in milligrams) per gram of the sample used for adsorption. The analysis results of iodine adsorption values included a total of 21 samples. These samples comprised 4 carbonization process samples, 4 samples activated using a 1-step process, 4 samples activated with wet powder using a 2-step process, 4 samples activated with bulk wet using a 2-step process, 4 samples activated with dry powder using a 2-step process, and 1 sample of commercial activated carbon. The experimental results indicated that the samples produced using the carbonization process (CP/rwt, CP/rsp, CP/Lw, and CP/cs) had the lowest iodine adsorption values, ranging approximately from 122 to 193 mg I_2/g of sample, as shown in **Figure 3(a)**. Activated carbon obtained using a 1-step activation process (AC/rwt, AC/rsp, AC/Lw, and AC/cs), where raw wood is soaked in a NaOH solution before being incinerated, tends to have higher iodine adsorption values, ranging from 209 to 347 mg I2/g of sample, as shown in **Figure 3(b)**. The enhanced iodine adsorption capacity of these samples is due to the chemical activation, which promotes the development of a more porous structure, increasing the surface area and thereby enhancing the material's adsorption potential.

The results of the 2-step activation experiment, which involved mixing carbonized carbon samples with NaOH solution, showed that the samples activated with bulk wet using a 2-step process exhibited a slight increase in iodine adsorption compared to those activated with a 1-step process, as depicted in **Figure 3(c)**. This indicates that while the bulk wet 2-step process slightly improves the adsorption capacity, it is not as effective as the chemical activation method. The chemical activation method utilizing wet powder in a 2-step process, where carbonized carbon samples are finely ground and then mixed with NaOH solution before incineration, demonstrated a higher adsorption tendency. This resulted in increased iodine adsorption across all 4 types of starting materials (rubber wood twigs, rubber seed pods, Leucaena wood, and coconut shells) compared to activation with a 1-step process and bulk wet 2-step process, as shown in **Figure 3(d)**. The increased iodine absorption can be attributed to the finer particle size and greater surface area that allows for more efficient interaction with the NaOH solution during activation. However, the iodine adsorption values mentioned above have not yet met the industrial product standard for activated carbon outlined in the TIS 900 - 2004 standard by the Ministry of Industry of Thailand, which specifies that the iodine number should not be less than 600 mg I_2/g of the sample [1,4,13,14]. The results also revealed that activated carbon obtained from the 2-step process, activated with dry powder using powdered carbonized carbon samples obtained from rubber wood twigs (AC/rwt), exhibited a high iodine adsorption value. The highest value reached was 616.73 mg I_2/g of the sample, surpassing the criteria of the activated carbon industry product standard, TIS 900 - 2004. In comparison with commercial activated carbon (C/AC), it was observed that the iodine adsorption value of the commercial activated carbon was 743.77 mg I_2/g of the sample, as depicted in **Figure 3(e)**. This highlights that while the 2-step activation method produces activated carbon with promising iodine adsorption values, it is still lower than commercial-grade activated carbon, which is expected due to differences in production scale and optimization.

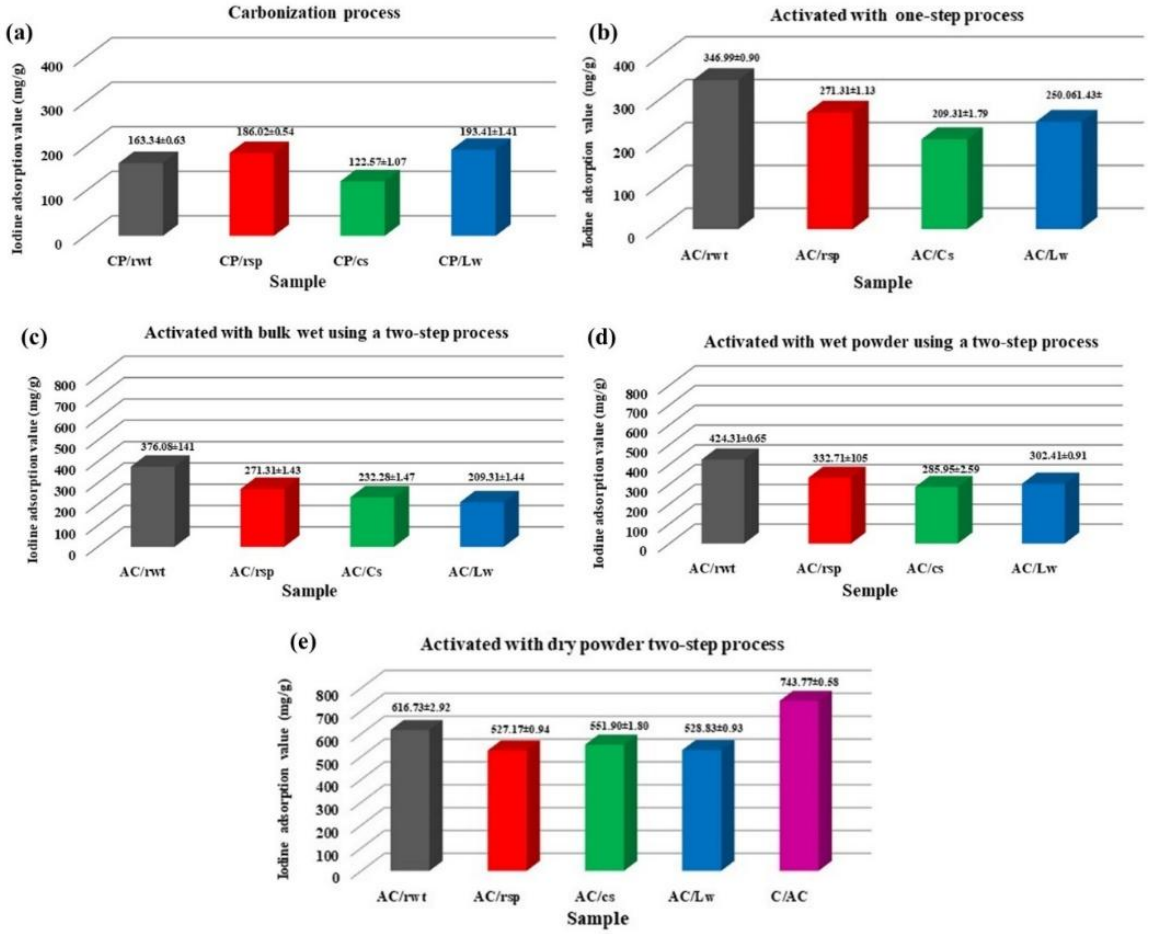

Figure 3 Iodine adsorption values (mg I_2/g sample) of (a) carbonization process samples (CP/rwt for rubber wood twigs, CP/rsp for rubber seed pods, CP/Lw for Leucaena wood, and CP/cs for coconut shells) and (b) samples activated using a 1-step process; (c) activated with bulk wet using a 2-step process, (d) activated with wet powder using a 2-step process, and (e) activated with dry powder using a 2-step process, when AC/rwt for rubber wood twigs, AC/rsp for rubber seed pods, AC/Lw for Leucaena wood, and AC/cs for coconut shells).

Based on the primary reactions that take place during activation with KOH, the studies by Mistar *et al.* [10] and Xu *et al.* [23] explain the mechanism of pore creation in activated carbon during the gasification process. However, in this research, NaOH was used as the activator in the pore formation process to produce activated carbon. This helps explain the mechanism of pore formation based on the findings reported, as shown in **Figure 4**. The infographic in **Figure 4**, illustrates the mechanism of pore formation on carbonized carbon using NaOH as the activating reagent. This process involves 4 main steps as detailed in previous reports [10,23,24]. In the first step, the decomposition of NaOH to produce Na_2O and H_2O typically occurs at a temperature of around 320 °C. Then, the Na_2O precursor reacts with the surface of the carbonized carbon (C) to form metallic Na and release CO gas at a temperature of around 800 °C, which provides porosity dispersion. In the second pathway, the H_2O molecules from the decomposition of NaOH react with the surface of the C to generate CO and H_2 gas. This reaction typically occurs at temperatures above 700 °C and is known as the water-gas shift reaction.

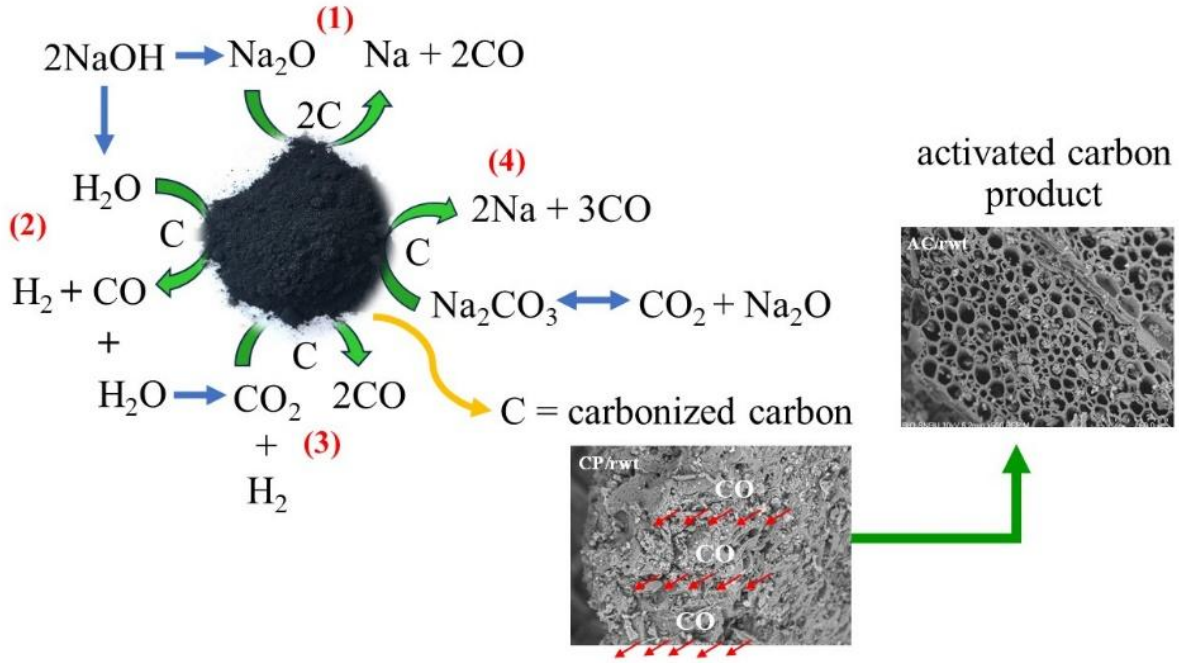

Figure 4 Infographic illustrating the proposed reaction mechanism for pore formation in carbonized carbon when activated with NaOH as the activating reagent.

Additionally, some molecules of CO gas in pathway of the reaction 1 or 2 can be reacted with H_2O to produce CO_2 molecules typically occurs at temperatures between 200 - 400 °C and is known as the water-gas shift reaction. Then this CO_2 molecule will react against the surface of the C to generate CO gas generally occurs at temperatures between 700 and 1000 °C, and is known as the Boudouard reaction. The CO gas comes off the surface of the carbonized carbon, causing another form of formation which is considered a third mechanism. The fourth possible reaction mechanism to generate porosity on the surface of carbonized carbon involves some molecules of Na_2O (from pathway 1) reacting with CO_2 molecules (from pathway 3) to generate Na_2CO_3. This reaction typically occurs at temperatures around 500 to 600 °C. Then, the Na_2CO_3 precursor will react with the C to produce CO gas, which is released from the surface of the carbonized carbon, leading to the generation of pores on its surface area. This reaction typically occurs at temperatures above 800 °C and is known as the decomposition or thermal decomposition of sodium carbonate. These 4 pathway reaction mechanisms contribute to the formation of pores on the surface of carbonized carbon, resulting in increased surface area and porosity, which is consistent with the results of the iodine adsorption value analysis of the samples shown in **Figure 3** [10,23,24]. This increased surface area and porosity are highly desirable in various applications such as adsorption, catalysis, and energy storage, as they enhance the material's ability to interact with gases, liquids, and other substances.

In this research, an innovative simple biomass incinerator was used to maintain temperatures between 600 - 800 °C for 2 h which is crucial for reactions at the carbon surface. The analysis of iodine adsorption values showed that raw wood material, incinerated without an activating reagent, had the lowest porosity and iodine adsorption values. Activated carbon produced using a 1-step activation process (soaking raw wood in NaOH before incineration) had higher iodine adsorption values than those from the carbonization process alone. However, the strong bonds in the chemical structure of raw wood materials (cellulose, hemicellulose, and lignin) made pore creation challenging, resulting in low porosity and iodine adsorption values that did not meet the standard [10,14,25-27]. In the preparation of activated carbon using a 2-step process, it was found that mixing carbonized carbon samples that had not been powdered with a NaOH solution showed a slight increase in iodine adsorption compared to the 1-step process. This is because the large size of the carbonized

carbon samples causes poor mixing with the NaOH solution. Conversely, the method utilizing wet powder in a 2-step process, where powdered carbonized carbon samples are mixed with a NaOH solution, exhibited significantly increased iodine adsorption across all 4 types of starting materials. This improved result can be attributed to the smaller particle size of the powdered carbonized carbon, which enhances the homogeneity of the mixture with the NaOH solution. The smaller size allows for a more uniform distribution of NaOH on the surface of the carbon particles, promoting more effective chemical reactions during the activation process. Specifically, the smaller particles increase the surface area available for reaction, facilitating the formation of more pores and enhancing the overall surface reactivity. This aligns with the 4 reaction mechanisms proposed for pore formation during the activation process, where the interaction between NaOH and the carbonized carbon leads to the breakdown of carbon structures, generation of new surface area, and creation of micropores. These mechanisms are particularly enhanced when using finer powders, as the increased surface area of smaller particles allows for better interaction with NaOH, resulting in higher porosity and iodine adsorption values. This outcome is in contrast to larger, less reactive particles, where the surface interactions are less effective, leading to lower iodine adsorption.

On the other hand, using a 2-step process with dry powder for the production of activated carbon indicated a higher iodine adsorption value compared to the results of previous experiments. Especially, the sample of AC/rwt derived from rubber wood twigs displayed the highest iodine adsorption value and met the criteria of the activated carbon industry product standard. The reason for this result may be that mixing NaOH in the solid state with the powdered carbonized carbon sample using a grinding method caused the NaOH to adhere to the carbonized carbon surface. Then, when heated to a high temperature, a reaction occurs that creates pores on the carbonized surface, increasing the surface pore density. This is consistent with the reaction mechanism shown in **Figure 4**. The 4 starting materials namely rubber wood twigs, rubber seed pods, Leucaena wood, and coconut shells possess distinct chemical compositions and structures. Consequently, when they are transformed into carbonized carbon samples, they exhibit varied properties including the hardness of the contact surface. This disparity may lead to differences in the pore formation reaction on the surface of the 4 starting carbonized carbon samples resulting in distinct pore quantities. These differences directly influence the iodine adsorption efficiency mentioned [14,22,23,26].

The BET surface area analysis

Identifying the pore structure of activated carbon is crucial prior to designing its applications. The Brunauer-Emmett Teller (BET) method serves as a fundamental approach to calculate the specific surface area of activated carbon based on its isotherms. Inert gas adsorption, commonly utilizing nitrogen (N_2), is favored due to its ability to reveal scientific insights into the textural characteristics of activated carbon. **Figure 5**, displays the N_2 adsorption isotherms obtained at 77 K for all synthesized carbonized carbon and activated carbon which prepared using various methods and activation temperatures. Additionally, **Table 1** presented the results of the analysis of BET surface area, pore volume, and average pore diameter. The experimental results indicated that the N_2 gas adsorption isotherm of carbonized carbon samples typically exhibited the lowest nitrogen gas adsorption values, as illustrated in **Figure 5(a)**. However, samples subjected to activation, including those activated via a 1-step process (**Figure 5(b)**), a 2-step process with bulk wet activation (**Figure 5(c)**), a 2-step process with wet powder activation (**Figure 5(d)**), and a 2-step process with dry powder activation (**Figure 5(e)**), generally showed an increased N_2 gas adsorption isotherm. Moreover, activated carbon produced through the 2-step process with dry powder activation tends to display the highest nitrogen gas adsorption isotherm among the tested materials.

After pore volume, average pore diameter, and BET surface area analysis, it was shown that the AC/rwt sample that was produced using a 2-step procedure with dry powder activation had the greatest BET surface area value, at 726.60 m^2/g. Following this, the AC/cs sample showed a value of 711.24 m^2/g, the AC/Lw sample had a value of 586.37 m^2/g, and the AC/rsp sample had a value of 520.99 m^2/g, respectively. Compared to all the activated carbon samples generated in this study, the commercially available sample (C/AC) showed a very high BET surface area value of 995.02 m^2/g. These

results indicate a clear relationship between the surface area and the iodine adsorption values reported in **Figure 3**. However, by definition, activated carbon needs to have a surface area per mass ratio (usually between 600 and 2,400 m^2/g) that is much larger than that of regular charcoal, meaning that it must have a porous structure [1,3,5,10,14]. From the results of the N_2 gas adsorption analysis, it was found that the AC/rwt sample obtained through both a 2-step process with dry powder activation and a 2-step process with wet powder activation, as well as the AC/cs sample derived from a 2-step process with dry powder activation, have a surface area per mass value that meets the activated carbon standard criteria. In contrast, the other samples, including AC/Lw and AC/rsp, exhibited surface area values below 600 m^2/g, thus failing to meet the minimum surface area requirement for activated carbon. This highlights the insufficient pore development in these samples, which affects their adsorption performance and overall effectiveness.

Table 1 Comparison of the BET surface area, pore volume and average pore diameter of the sample derived from (1) carbonized carbon, (2) activated with 1-step process, (3) activated with bulk wet using a 2-step process, (4) activated with wet powder using a 2-step process, (5) activated with dry powder 2-step process, and (6) C/AC.

Sample	BET surface area (m^2/g)	Total pore volume (cm^3/g)	Average pore diameter (nm)
(1) carbonization process			
1.1 CP/rwt	25.7512	0.0220	3.4105
1.2 CP/rsp	50.9923	0.0409	3.2114
1.3 CP/cs	1.0442	0.0071	2.7336
1.4 CP/Lw	4.5221	0.0092	2.6631
(2) activated with 1-step process			
2.1 AC/rwt	96.4211	0.1380	5.7241
2.2 AC/rsp	256.7743	0.2562	3.9915
2.3 AC/cs	174.0100	0.1721	3.9559
2.4 AC/Lw	197.7500	0.1323	2.6767
(3) activated with bulk wet using a 2-step process			
3.1 AC/rwt	442.2633	0.2212	2.0006
3.2 AC/rsp	392.2338	0.2435	5.5429
3.3 AC/cs	218.0126	0.3151	5.7816
3.4 AC/Lw	379.4918	0.2033	2.1425
(4) activated with wet powder using a 2-step process			
4.1 AC/rwt	678.7707	0.2875	3.5168
4.2 AC/rsp	402.1703	0.2057	2.0457
4.3 AC/cs	449.7025	0.2305	2.0498
4.4 AC/Lw	393.5546	0.2033	2.0659
(5) activated with dry powder 2-step process			
5.1 AC/rwt	726.6028	0.3748	2.0635
5.2 AC/rsp	520.9905	0.3316	2.5462
5.3 AC/cs	711.2402	0.3592	2.0203
5.4 AC/Lw	586.3700	0.3197	2.1812
(6) C/AC	995.0223	0.8367	3.3637

Note: 1) The BET surface area, pore volume, and average pore diameter of activated carbon should fall within the ranges of 600 to 2400 m^2/g for surface area and 0.20 to 1.00 cm^3/g for pore volume, as reported in previous research studies [1,3,5,10,14].

2) The results obtained from the analysis using the BET-sorp mini II, manufactured by BEL, Japan, have high accuracy, with an uncertainty range of ± 1 - 2 %.

Therefore, the results of this experiment indicate that the synthesized activated carbon met the standard criteria for surface area per mass in 3 out of the total 20 samples, as shown by the data in **Table 1**. This finding supports previous research highlighting the importance of surface area in determining the adsorption capacity of activated carbon. Specifically, 3 samples—AC/rwt activated with both dry and wet powder—exhibited surface areas that met the minimum activated carbon standard of 600 m^2/g [1,3,5,10,14]. The data also aligns with studies that show higher iodine adsorption values correlate with higher surface area and increased porosity. The experiment reveals that activated carbon samples prepared through a 2-step process with dry powder activation generally exhibited higher total pore volumes compared to those prepared by other methods. This result is consistent with the pore formation mechanism outlined in **Figure 4**, which suggests that the NaOH solution and the powdered carbonized carbon interact more efficiently, allowing for better pore development. These findings also underscore the critical role of particle size in the activation process, as smaller particles provide a larger surface area for the NaOH solution to react with, resulting in the formation of smaller, more numerous pores. Interestingly, the AC/rwt samples activated with wet powder, while meeting the surface area standards, exhibited lower pore volumes and larger average pore diameters (ranging from 2.0203 to 2.1812 nm) compared to their dry powder counterparts. This discrepancy suggests that wet powder activation may primarily enlarge existing pores, rather than creating new ones. These findings are consistent with the notion that wet activation tends to increase pore size, while dry powder activation facilitates the creation of a higher number of smaller pores. Moreover, all samples exhibited average pore diameters that fell within the mesopore range (2 - 5 nm), as categorized under the IUPAC guidelines for pore classification. The nitrogen gas adsorption isotherms confirmed Type II behavior, which is typical for mesoporous materials. This behavior reflects the characteristic monolayer adsorption at low pressures, followed by multilayer adsorption as pressure increases. This observation further reinforces the idea that the activated carbon samples possess a mesoporous structure suitable for adsorption applications.

In addition to the surface area and pore volume data, scanning electron microscopy (SEM) analysis provided valuable insights into the morphology of the activated carbon samples. SEM images helped confirm the presence and distribution of mesopores, offering visual evidence that supported the nitrogen adsorption data. The SEM images also confirmed how various activation methods influenced pore structure, leading to a more thorough understanding of the material characteristics. Overall, these results underscored the significant influence of activation methods on pore characteristics, which in turn affected the adsorption performance of activated carbon. As demonstrated in this study, activation methods that optimized surface area and pore volume, such as dry powder activation, were more effective in enhancing the adsorption capacity, making them more suitable for applications like water purification and air filtration [10,11,26-29].

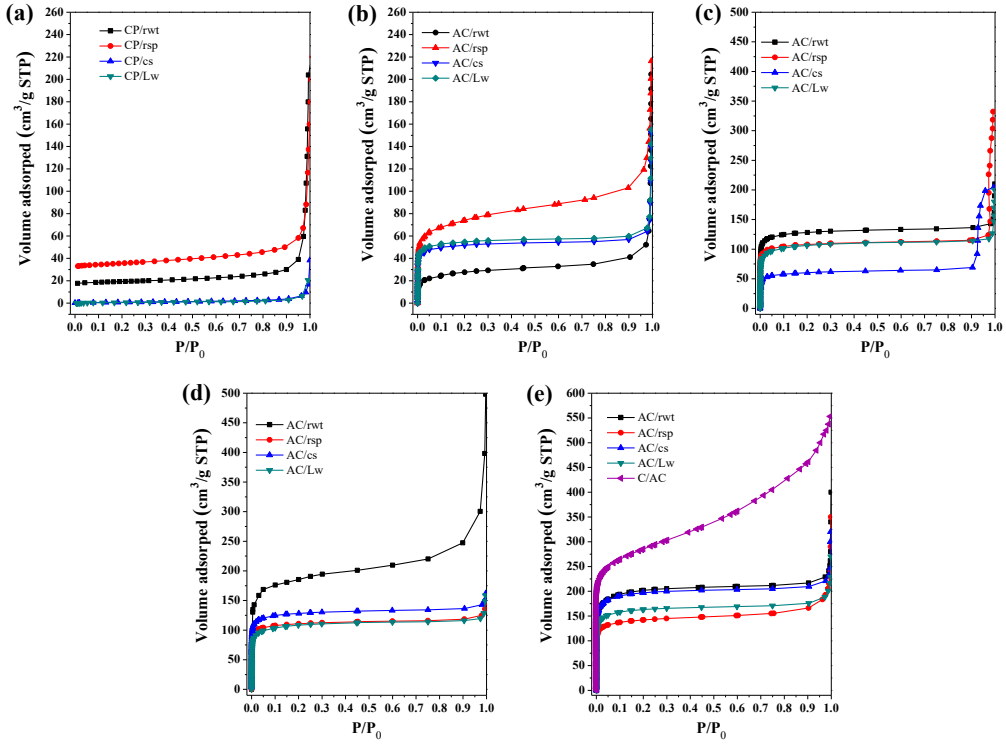

Figure 5 The N_2 adsorption isotherms at 77 K of the sample derived from (a) carbonization process, (b) activated with 1-step process, (c) activated with bulk wet using a 2-step process, (d) activated with wet powder using a 2-step process, and (e) activated with dry powder 2-step process.

Analysis of methylene blue adsorption values

The experiment aimed to determine the adsorption value of methylene blue in various samples. The study selected raw material samples that had undergone the carbonization process namely rubber wood twigs (CP/rwt) and coconut shells (CP/cs). For this purpose, CP/rwt et CP/cs were chosen. These were compared to activated carbon synthesized using a 2-step activation process with dry powder from rubber wood twigs (AC/rwt) and coconut shells (AC/cs). Based on experimental results from iodine adsorption determination and BET surface area analysis, it was found that the synthesized activated carbon of AC/rwt and AC/cs samples exhibited the highest values. Additionally, commercial activated carbon (C/AC) was included for comparison. The methylene blue adsorption analysis in this study follows the procedure outlined by Pathania *et al.* [22], as shown in **Figure 6**.

The results of the study showed that commercial activated carbon (C/AC) had the highest adsorption efficiency for methylene blue with an adsorption capacity of 100 ± 0.11 %. The AC/rwt activated carbon sample exhibited a methylene blue adsorption efficiency similar to that of commercial activated carbon with a value of 99.65 ± 0.24 %. The AC/cs activated carbon sample had a slightly lower methylene blue adsorption efficiency of 98.29 ± 0.52 %, compared to commercial activated carbon and AC/rwt activated carbon. The carbonization process samples both CP/rwt and CP/cs had methylene blue adsorption efficiencies of approximately 80 % as depicted in **Figure 6**. The trends in the iodine adsorption efficiency of each sample and the experimental results of the BET surface area mass analysis are in agreement with the methylene blue adsorption efficiency values. The results of this experiment are consistent with those reported by Roschat *et al.* [14], Ramalingam *et al.* [26], and Santoso *et al.* [29], who explained that the methylene blue adsorption efficiency value aligns with the surface area per unit mass of the sample. The higher the pore volume of the activated carbon sample, the higher the adsorption efficiency.

To ensure the accuracy and reliability of the methylene blue adsorption data presented in **Figure 6**, absorbance measurements were rigorously evaluated in accordance with the Beer–Lambert Law, which posits

that absorbance values exceeding 1.0 may compromise accuracy due to limited light transmittance at elevated analyte concentrations. Standard methylene blue solutions were prepared at various concentrations, and a preliminary assessment of the spectrophotometer's linear dynamic range was performed. The findings indicated that concentrations up to approximately 5 mg/L yielded absorbance values within a reliable range of 0.1 - 1.0. Samples exhibiting absorbance values beyond this threshold were appropriately diluted with deionized water to ensure consistency within the linear range. As a result, the standard calibration curve was refined to include only data points within the linear response interval, yielding a high correlation coefficient ($R^2 = 0.9999$), thereby minimizing analytical deviation and enhancing the reliability of the adsorption efficiency results.

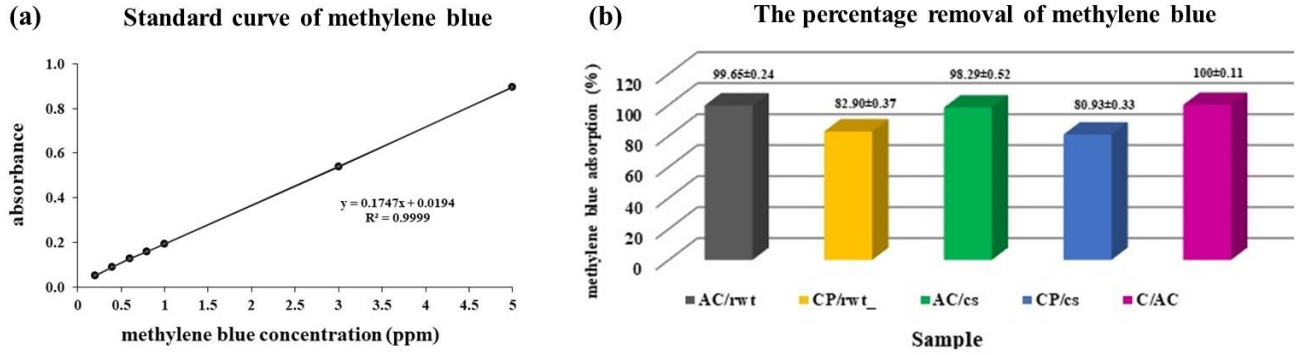

Figure 6 (a) standard curve of methylene blue and (b) the percentage removal of methylene blue.

Surface morphology analysis

Scanning electron microscope

The surface morphology of the samples derived from the carbonization process and the activated carbon samples obtained in this study was characterized using a scanning electron microscope (SEM). The results in **Figure 7** reveal that the carbonization process samples (CP/rwt, CP/rsp, CP/Lw, and CP/cs) exhibit distinct characteristics. The raw material charcoal samples, CP/rwt and CP/rsp, display rough surfaces with few pores, while CP/Lw and CP/cs samples have smoother surfaces with limited pore structures. These observations correspond with the BET analysis and iodine adsorption tests, showing that the raw charcoal samples exhibit low adsorption efficiency, which is attributed to their limited exposed surface area. In contrast, the results in **Figure 8** indicate that commercial activated carbon (C/AC) and the samples activated through the dry powder 2-step process (AC/rwt, AC/cs, AC/rsp, and AC/Lw) show pronounced porosity with a significant number of pores. SEM imaging of C/AC reveals relatively uniform and well-arranged pore sizes, while the AC/rwt and AC/cs samples exhibit consistent and orderly pore structures. On the other hand, AC/rsp and AC/Lw samples demonstrate irregular pore sizes and less organized pore structures.

The average pore sizes of the activated carbon samples were estimated using Scanning Electron Microscopy (SEM). SEM revealed that AC/rwt and AC/cs exhibited smaller, more uniform pores, while AC/rsp and AC/Lw showed larger and more irregularly shaped pores. The discrepancy between pore sizes observed in SEM images (micrometer scale) and data obtained from the BET analysis (nanometer scale) can be attributed to the different types of porosity each method measures. BET analysis provides detailed insights into micropores and mesopores, which are critical for gas adsorption, and focuses on porosity at the nanometer scale. The higher surface areas observed for AC/rwt and AC/cs in the BET analysis are likely due to their more uniform, well-formed pores, which directly correlate with enhanced iodine adsorption efficiency. In contrast, SEM imaging operates at a larger scale, revealing visible surface features such as macropores and surface roughness. While these features may not directly contribute to adsorption, they provide valuable information about the material's surface morphology. SEM captures larger pores and structural irregularities

that differ from the fine internal porosity measured by BET analysis, which is crucial for adsorption processes.

The differences in pore size and distribution observed between SEM and BET analyses suggest that a uniform, well-developed pore structure, as indicated by the BET results, plays a significant role in enhancing adsorption performance. The complementary nature of both techniques highlights the importance of both nanometer-scale porosity and larger-scale surface features in determining the material's adsorption efficiency. A well-structured pore network, particularly within the mesopore and micropore ranges, contributes to improved iodine adsorption and likely enhances the adsorption of other molecules as well. The formation of these pores is driven by the gasification process during the activation with NaOH, as depicted in **Figure 4**. This reaction mechanism contributes significantly to the efficiency of the activated carbon in absorbing various substances. These findings support the previous studies by Mistar *et al.* [10], Xu *et al.* [11], Roschat [14], and Ahmed and Theydan [30], which report similar pore formation mechanisms during the activation process.

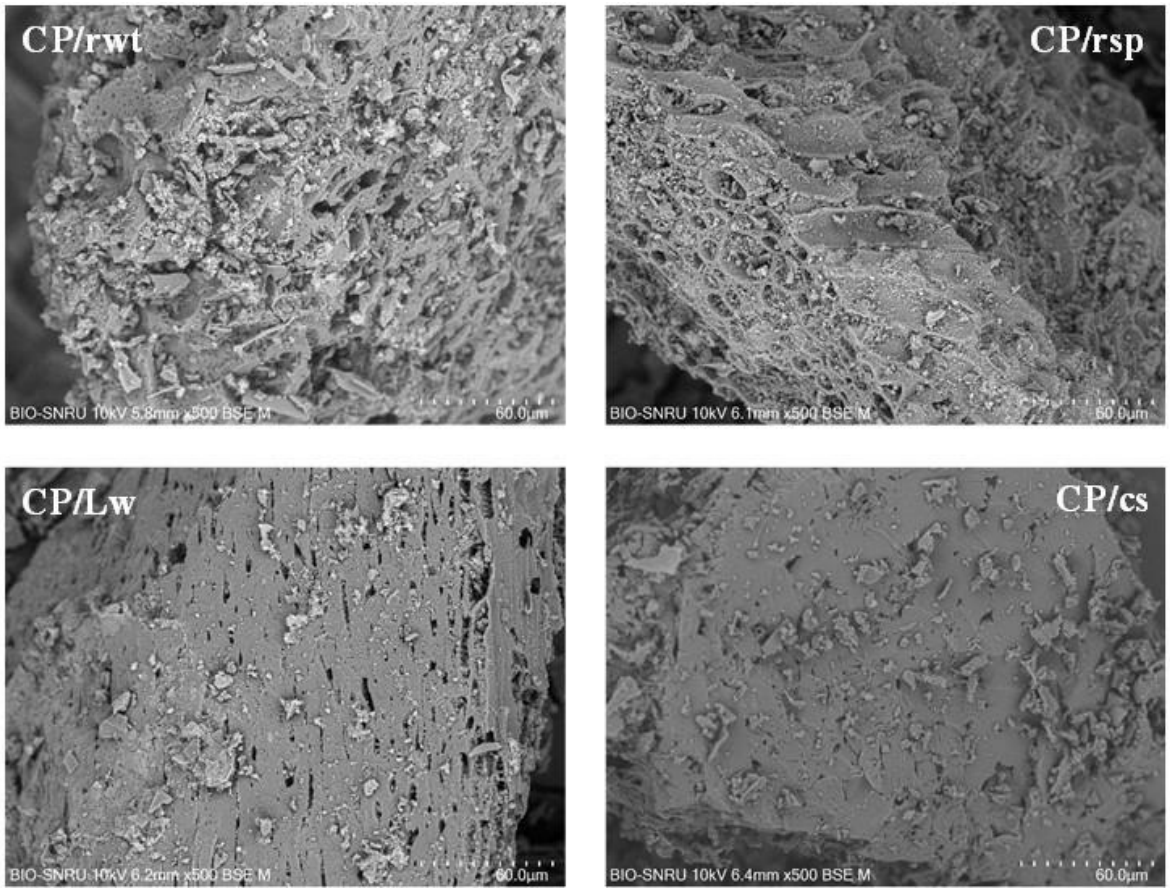

Figure 7 SEM images of the samples derived from the carbonization process with the following symbols: CP/rwt for rubber wood twigs, CP/rsp for rubber seed pods, CP/Lw for Leucaena wood, and CP/cs for coconut shells.

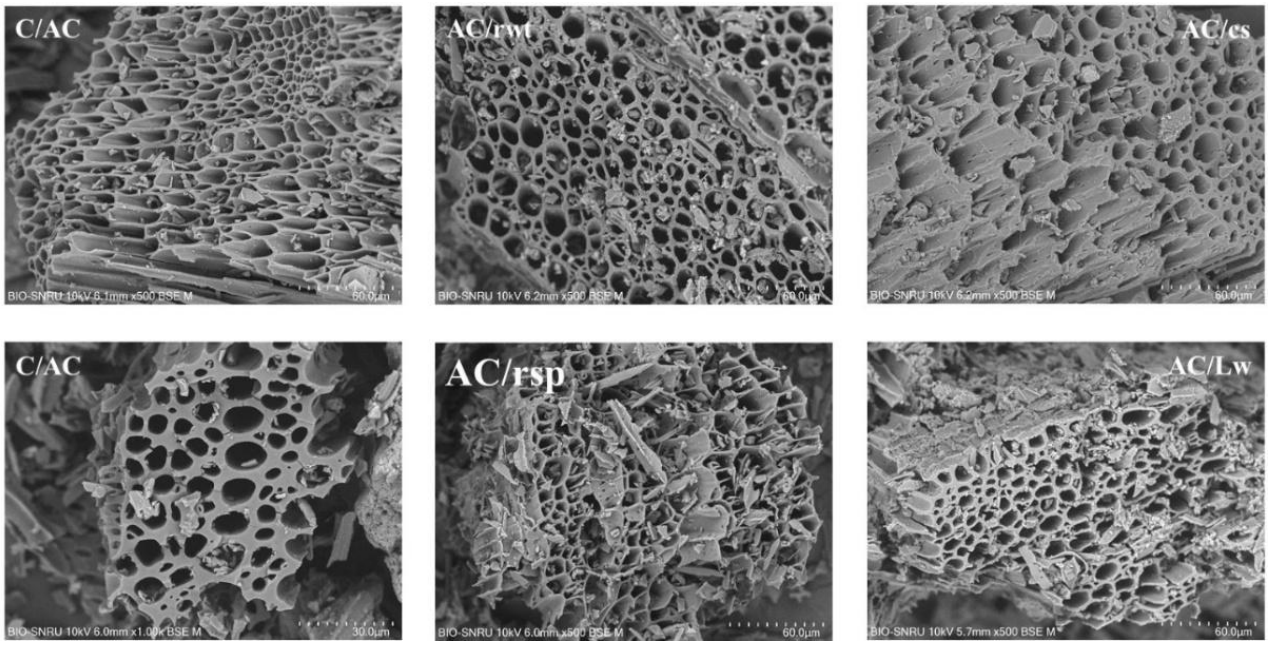

Figure 8 SEM images of the samples derived from the activated with dry powder 2-step process from rubber wood twigs (AC/rwt), coconut shells (AC/cs), rubber seed pods (AC/rsp), and Leucaena wood (AC/Lw) compared with commercial activated carbon (C/AC).

Transmission electron microscope

The morphological and structural studies of the AC/rwt and AC/cs samples, compared with C/AC and CP/rwt samples, were conducted using a transmission electron microscope (TEM), as shown in **Figure 9**. The TEM images revealed that the C/AC sample has a well-defined distribution of pores and channels resulting in high electron beam transmission. These findings are consistent with the results from the BET technique analysis, adsorption efficiency tests for iodine and methylene blue, and SEM. The most heterogeneous surface morphology appears in the activated carbons post-activation. The single carbon layers shown in TEM micrographs are twisted and disorganized, with randomly interconnected graphite-like surfaces [31-33]. The AC/rwt sample prepared using a 2-step dry powder activation process from rubber wood twigs, produced experimental results similar to those of the C/AC sample. However, it can be observed that the AC/rwt sample has less porosity than the C/AC sample as evidenced by the lower electron beam transmission compared to the C/AC sample.

When considering the AC/cs sample, it was found that the electron beam transmission effect was less than that of both the C/AC and AC/rwt samples. This finding was in line with the BET surface area and the iodine and methylene blue adsorption efficiency tests of the AC/cs samples, which were lower than those of the C/AC and AC/rwt samples. In contrast, the carbonization process derived from rubber wood twigs (CP/rwt) resulted in minimal electron beam transmission leading to a rather dull TEM image. The results of this study are consistent with the BET surface area measurements and the adsorption efficiency tests for iodine and methylene blue, which indicated that the CP/rwt samples had fewer pores compared to the activated carbon samples. The results of the TEM analysis not only demonstrated the nature of pore formation and distribution in the samples but also supported the findings from BET surface area measurements, adsorption efficiency tests for iodine and methylene blue, and SEM. These analyses confirmed the mechanism of pore formation through gasification as previously discussed.

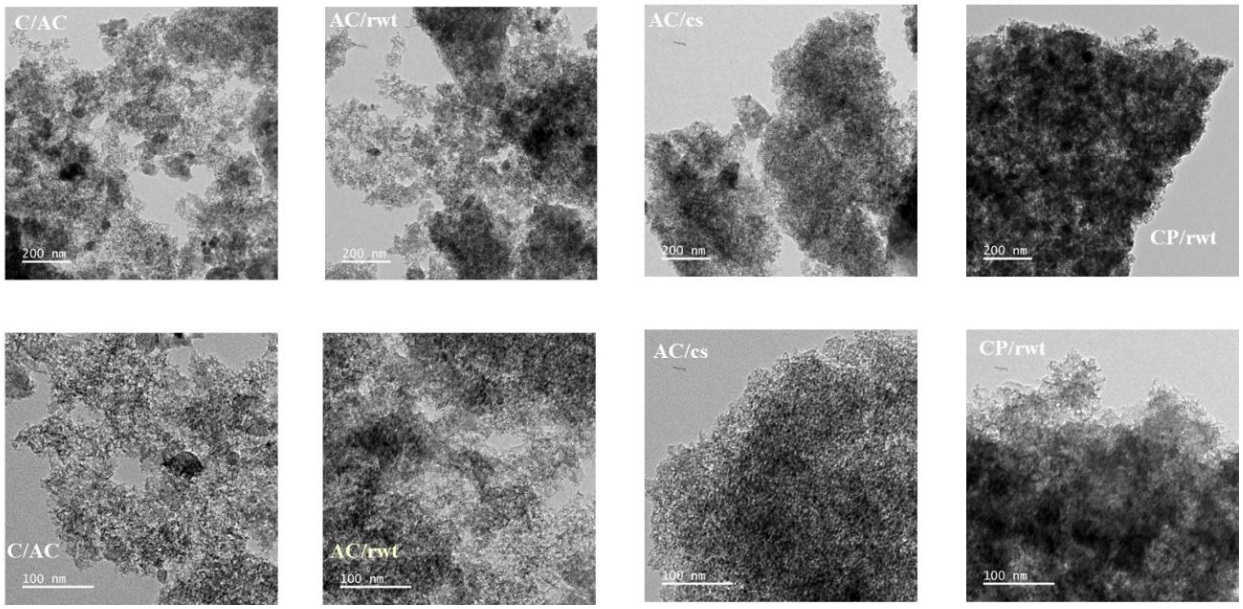

Figure 9 TEM images of the commercial activated carbon (C/AC) compared with the samples derived from the activated with dry powder 2-step process from rubber wood twigs (AC/rwt) and coconut shells (AC/cs), and the samples derived from the carbonization process derived from the rubber wood twigs (CP/rwt).

Energy Dispersive X-Ray Spectroscopy (EDS)

Energy Dispersive X-Ray Spectroscopy (EDS) analysis using the TEM image for elemental mapping was displayed in **Figure 10** and **Table 2**. The EDS results showed that the elemental composition of C/AC, AC/rwt, AC/cs, and CP/rwt samples primarily consisted of carbon (C) and oxygen (O) atoms, with calcium (Ca), magnesium (Mg), sodium (Na), and silicon (Si) present in minor amounts. This result is consistent with numerous studies that have reported carbon and oxygen as the main elements in activated carbon samples. These 2 elements are predominant in various plant parts, such as stems, branches, bark, and fruit peels, which are commonly used as starting materials in the production of activated carbon [34-36]. However, the experimental results showed variations in the carbon and oxygen contents across the samples. The C/AC sample contained approximately 53 % carbon and 43 % oxygen by weight. This may be due to the raw materials used to produce the C/AC samples. The carbon content was not very high because, during the activation process, some carbon was converted to CO gas, creating large pores. This resulted in the activated carbon product having a lower carbon content compared to other samples.

Table 2 The EDS data for elemental analysis of the elemental analysis of C/AC, AC/rwt, AC/cs, and CP/rwt.

Sample	Element (Weight %)					
	C	O	Ca	Mg	Na	Si
C/AC	53.21	42.86	1.55	0.30	1.66	0.42
AC/rwt	68.84	25.60	1.05	0.95	1.34	2.22
AC/cs	69.57	26.60	0.87	0.75	1.08	1.13
CP/rwt	73.35	21.60	1.31	0.92	0.77	2.05

Note: The results obtained from the elemental analysis using Energy Dispersive X-ray Spectroscopy (EDS) have high accuracy, with an uncertainty range of ± 1 - 2 %.

The experimental results were consistent with the characteristics and number of pores observed in the C/AC samples. Meanwhile, the AC/rwt and AC/cs samples had similar carbon and oxygen contents, approximately 69 and 26 % by weight, respectively. In the CP/rwt sample, the carbon and oxygen contents were

found to be approximately 73 and 22 % by weight, respectively. Such experimental data can be used to explain that the amount of carbon and oxygen, which are key chemical elements, depends on the nature of the starting materials used in the production of activated carbon. Many studies have reported that the carbon and oxygen contents in activated carbon typically vary within the ranges of approximately 60 - 80 and 20 - 40 % by weight, respectively [10,37,38]. In addition, it is worth noting that the CP/rwt samples contained higher amounts of carbon and oxygen compared to the activated carbon samples. This could be because the CP/rwt samples undergo only 1 heating step in the carbonization process resulting in less carbon loss. In contrast, the activated carbon samples undergo the KOH activation process which produces CO gas during the pore formation reaction.

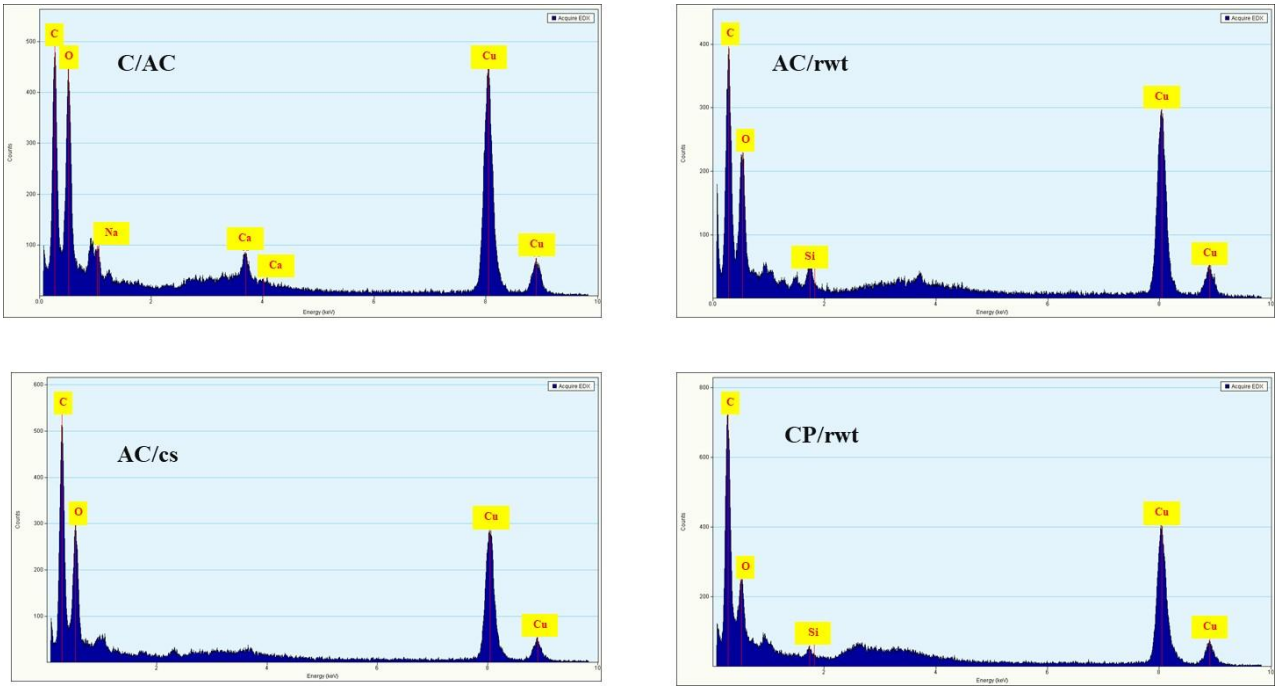

Figure 10 The EDS data for elemental analysis of the commercial activated carbon (C/AC) compared with the samples derived from the activated with dry powder 2-step process from rubber wood twigs (AC/rwt) and coconut shells (AC/cs), and the samples derived from the carbonization process derived from the rubber wood twigs (CP/rwt).

FT-IR analysis

Figure 11(a) displays the findings of the identification study that combined chemical analysis and the Fourier transform infrared (FT-IR) functional group analysis technique. The FT-IR spectra of samples CP/rwt, CP/cs, AC/rwt, AC/cs, and C/AC showed similar vibrational characteristics of functional groups. All of the samples' spectra revealed bond vibrations that might correspond to C=C functional groups (aromatic compounds) at wavenumbers around 1580 - 1560 cm^{-1}, while the vibrations of other types of functional groups were not evident. This is because the raw carbon samples CP/rwt and CP/cs, as well as the activated carbon samples AC/rwt, AC/cs, and C/AC, primarily consist of carbon, which forms strong bonds between carbon atoms. As a result, the functional groups of various types of organic compounds are not clearly visible. However, the C=C functional groups may arise from organic substances present in the starting materials such as cellulose and lignin compounds which may leave some residues during the combustion process and are found in only small amounts. The study's findings concurred with those published by Foo and Hameed [39], Pouretedal and Sadegh [40], Mistar *et al.* [10], Dao *et al.* [25], and Roschat *et al.* [14]. These studies analyzed the chemical structure of the functional groups in activated carbon samples using FT-IR. They found that the functional groups present varied depending on the raw materials and preparation methods used for the activated carbon samples. Most of the functional groups

identified in organic compounds from plants include O–H stretching vibrations of hydroxyl groups, C–H stretching vibrations in methylene and methyl groups, C=C stretching vibrations of alkene, and C=O stretching vibrations of carboxyl, lactone, aldehyde, and ketone groups. These functional groups were found to correspond to the main chemical components of plants including cellulose, hemicellulose, and lignin.

XRD analysis

Figure 11(b) shows the XRD patterns of CP/rwt, CP/cs, AC/rwt, AC/cs, and C/AC samples. The results indicated that all samples primarily exhibited an amorphous solid structure. However, slight peaks indicating the presence of crystalline solids were also observed in all samples. These crystalline structures might have developed during the carbonization and chemical activation procedures, which required heating for 2 h at temperatures between 600 and 800 °C using an innovative simple biomass incinerator. This heating process may cause the amorphous carbon structure to change, leading to the formation of graphite carbon crystals, with a peak observed at approximately 2θ = 26.37 ° (XRD patterns of JCPDS 41-1487) [14,25,41-43]. Additionally, peaks corresponding to alkaline metals, which could be impurities or components of the starting materials, were found at 2θ positions of approximately 43.98, 49.05, 64.40, and 77.40 ° (XRD patterns of JCPDS 04-013-4058, JCPDS 04-0829, JCPDS 04-0835, and JCPDS 01-070-0392). The presence of these peaks in small amounts is consistent with the EDS data from the elemental analysis of the samples. Calcium, magnesium, sodium, and silicon are found in all parts of plants as a result of mineral accumulation. The amount of nutrients that plants absorb may vary depending on the mineral content of the soil in each area [44-46]. Consequently, the activated carbon obtained is primarily composed of disorganized amorphous carbon with widespread pores. These chemical structures and various properties are the hallmarks of the activated carbon obtained from this research in its application as an adsorbent, demonstrating high adsorption efficiency comparable to commercial activated carbon.

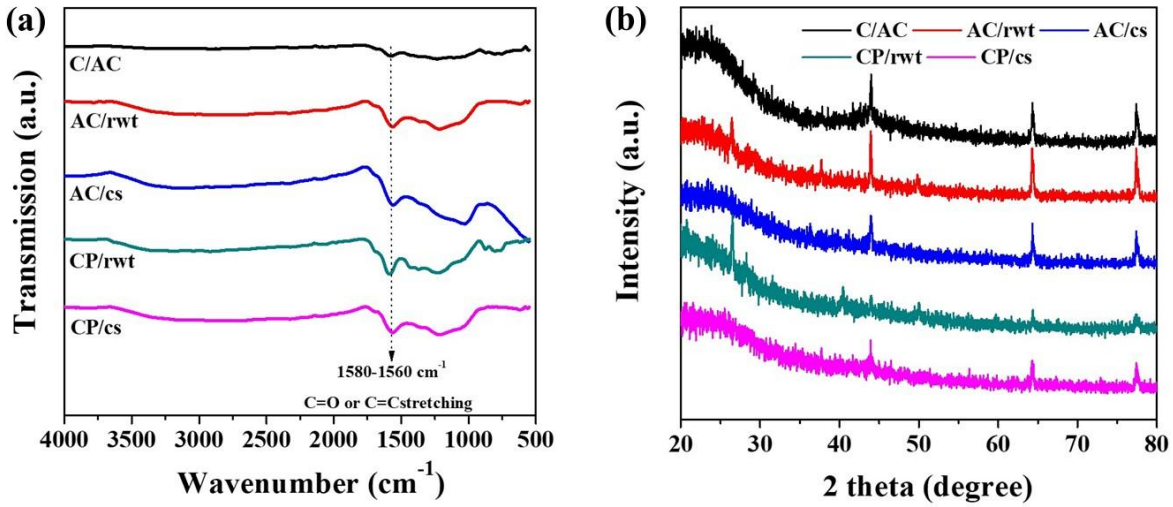

Figure 11 (a) The FT-IR analysis and (b) XRD analysis of the commercial activated carbon (C/AC) compared with the samples derived from the activated with dry powder 2-step process from rubber wood twigs (AC/rwt) and coconut shells (AC/cs), and the samples derived from the carbonization process derived from the rubber wood twigs (CP/rwt) and coconut shells (CP/cs).

Conclusions

This study successfully demonstrated the synthesis of activated carbons from agricultural waste materials, including rubber wood twigs, rubber seed pods, *Leucaena leucocephala* wood, and coconut shells. Both dry and wet chemical activation methods using NaOH, applied through an innovative biomass incinerator, were explored. The results revealed that activated carbon derived from rubber wood twigs (AC/rwt) via dry activation exhibited the best chemical and physical adsorption properties. The BET surface area analysis indicated a high porosity of 726.60 m^2/g, while the iodine number of 616.73 mg/g surpassed the industrial standard for activated carbon (TIS 900 - 2547). Elemental analysis confirmed carbon as the dominant element in the AC/rwt sample, and its methylene blue adsorption efficiency reached 99.65 %. The pore size distribution was characterized by mesoporous structures, with pore sizes ranging from 2 to 50 nm, as indicated by a Type II isotherm. Although the commercial activated carbon outperformed in certain metrics, such as surface area (950.02 m^2/g), iodine number (743.77 mg/g), and methylene blue adsorption (100 %), the results confirmed that agricultural waste can be effectively utilized to produce high-quality activated carbon. The synthesized activated carbon from rubber wood twigs met the required standards for iodine adsorption and demonstrated high methylene blue adsorption efficiency. These findings highlight the potential of agricultural waste materials as valuable resources for sustainable activated carbon production, offering a viable alternative for various adsorbent applications.

Acknowledgements

This project was funded by the National Research Council of Thailand (NRCT) (No. N42A650196) and the Innovation in Chemistry for Community Research Unit, Faculty of Science and Technology, Sakon Nakhon Rajabhat University, Thailand. The authors also express their gratitude to the Program of Chemistry, Faculty of Science and Technology, and the Biomass Energy Research Laboratory under the Center of Excellence on Alternative Energy, Sakon Nakhon Rajabhat University, Thailand, for providing the necessary equipment and tools for this project.

Declaration of Generative AI in Scientific Writing

During the preparation of this manuscript, the authors utilized ChatGPT to assist with English grammar checking. The authors thoroughly reviewed, revised, and edited the manuscript following the use of this tool. The authors accept full responsibility for the integrity and accuracy of the content presented in this publication.

CRediT author statement

Tappagorn Leelatam: Conceptualization; Formal analysis; Data curation; Investigation. **Wuttichai Roschat**: Conceptualization; Formal analysis; Data curation; Investigation; Writing - Original draft preparation; Writing – Reviewing and Editing. **Thanaphon Fongwichai**: Resources; Methodology; Investigation; Formal analysis. **Warisara Tamprasee**: Resources; Methodology; Investigation; Formal analysis. **Sunti Phewphong**: Resources; Methodology; Investigation; Formal analysis. **Preecha Moonsin**: Formal analysis; Data curation; Methodology. **Prawit Nuengmatcha**: Supervision; Formal analysis; Data curation; Writing – Reviewing and Editing. **Prawit Suwannarong**: Formal analysis; Data curation; Writing – Reviewing and Editing. **Vinich Promarak**: Supervision; Funding acquisition; Data curation; Writing – Reviewing and Editing.

References

[1] Y Ngernyen and K Kamwilaisak. Activated carbon from Thailand's biomass: A review literature. *Engineering and Applied Science Research* 2014; **40(2)**, 267-283.

[2] N Khadhri, MEK Saad, MB Mosban and Y Moussaoui. Batch and continuous column adsorption of indigo carmine onto activated carbon derived from date palm petiole. *Journal of Environmental Chemical Engineering* 2019; **7(1)**, 102775.

[3] K Kusmierek, A Swiątkowski, T Kotkowski, R Cherbanski and E Molga. Adsorption on activated carbons from end-of-life tyre pyrolysis for environmental applications. Part II. Adsorption from aqueous phase. *Journal of Analytical and Applied Pyrolysis* 2021; **158**, 105206.

[4] A Jantaboot, A Bunkham and P Aggarangsi. Production of activated carbon from corncob by combined phosphoric acid and carbon dioxide activation. *Thai Science and Technology Journal* 2023; **31(5)**, 94-107.

[5] N Muttil, S Jagadeesan, S Chanda, M Duke and SK Singh. Production, types, and applications of activated carbon derived from waste tyres: An overview. *Applied Sciences* 2023; **13(1)**, 257.

[6] C Bouchelta, MS Medjram, O Bertrand and J Bellat. Preparation and characterization of activated carbon from date stones by physical activation with steam. *Journal of Analytical and Applied Pyrolysis* 2008; **82(1)**, 70-77.

[7] MJ Prauchner and F Rodriguez-Reinoso. Chemical versus physical activation of coconut shell: A comparative study. *Microporous and Mesoporous Materials* 2012; **152**, 163-171.

[8] AA Ceyhan, O Sahin, O Baytar and C Saka. Surface and porous characterization of activated carbon prepared from pyrolysis of biomass by two-stage procedure at low activation temperature and its adsorption of iodine. *Journal of Analytical and Applied Pyrolysis* 2013; **104**, 378-383.

[9] H Hadoun, Z Sadaoui, N Souami, D Sahel and I Toumert. Characterization of mesoporous carbon prepared from date stems by H_3PO_4 chemical activation. *Applied Surface Science* 2013; **280**, 1-7.

[10] EM Mistar, T Alfatah and MD Supardan. Synthesis and characterization of activated carbon from Bambusa vulgaris striata using two-step KOH activation. *Journal of Materials Research and Technology* 2020; **9(3)**, 6278-6286.

[11] J Xu, J Yu, J Xu, C Shi, W Hu, J Hu and G Li. High-value utilization of waste tires: A review with focus on modified carbon black from pyrolysis. *Science of The Total Environment* 2020; **742**, 140235.

[12] I Jones, M Zhang, J Zhang, Z Zhang, J Penteado, J Gu and D Zhang. The application of spent tyre activated carbons as low-cost environmental pollution adsorbents: A technical review. *Journal of Cleaner Production* 2021; **312**, 127566.

[13] A Thammayod, W Roschat, T Leelatam, S Phewphong, B Maneerat, N Leelatam, A Thangthong, P Moonsin and V Promarak. Development of high-quality organic fertilizer from biomass waste and the application of biochar in local areas of Sakon Nakhon Province, Northeastern Thailand. *Trends in Sciences* 2025; **22(2)**, 9105.

[14] W Roschat, S Donrussamee, P Smanmit, S Jikjak, T Leelatam, S Phewphong, K Namwongsa, P Moonsin and V Promarak. Quality improvement of crude glycerol from biodiesel production using activated carbon derived from Krabok (*Irvingia malayana*) seed shells. *Korean Journal of Materials Research* 2024; **34(1)**, 1-11.

[15] AR Tobi, JO Dennis, HM Zaid, AA Adekoya and U Fahad. Comparative analysis of physiochemical properties of physically activated carbon from palm bio-waste. *Journal of Materials Research and Technology* 2019; **8(5)**, 3688-3695.

[16] V Yang, RA Senthil, J Pan, A Khan, S Osman, L Wang, W Jiang and Y Sun. Highly ordered hierarchical porous carbon derived from biomass waste mangosteen peel as superior cathode material for high performance supercapacitor. *Journal of Electroanalytical Chemistry* 2019; **855**, 113616.

[17] AL Cazetta, AMM Vargas, EM Nogami, MH Kunita, MR Guilherme, AC Martins, TL Silva, JCG Moraes and VC Almeida. NaOH-activated carbon of high surface area produced from coconut shell: Kinetics and equilibrium studies from the methylene blue adsorption. *Chemical Engineering Journal* 2011; **174(1)**, 117-125.

[18] T Sarawanan, NS Mahat, MN Rusli and MAA Zaini. Two-stage adsorber optimization of NaOH-prewashed oil palm empty fruit bunch activated carbon for methylene blue removal. *Chemical Product and Process Modeling* 2023; **18(3)**, 383-390.

[19] MA Yahya, CW Zanariah, CW Ngah, MA Hashim and Z Al-Qodah. Preparation of activated carbon from desiccated coconut residue by chemical activation with NaOH. *Journal of Materials Science Research* 2016; **5(1)**, 24-31.

[20] TA Khan, R Rahman and EA Khan. Adsorption of malachite green and methyl orange onto waste tyre activated carbon using batch and fixed-bed techniques: Isotherm and kinetics modeling.

Modeling Earth Systems and Environment 2017; **3**, 38.

[21] S Lv, C Li, J Mi and H Meng. A functional activated carbon for efficient adsorption of phenol derived from pyrolysis of rice husk, KOH-activation and EDTA-4Na-modification. *Applied Surface Science* 2020; **510**, 145425.

[22] D Pathania, S Sharma and P Singh. Removal of methylene blue by adsorption onto activated carbon developed from Ficus carica bast. *Arabian Journal of Chemistry* 2017; **10(1)**, S1445-S1451.

[23] Z Xu, J Chen, X Zhang, Q Song, J Wu, L Ding, C Zhang, H Zhu and H Cui. Template-free preparation of nitrogen-doped activated carbon with porous architecture for high-performance supercapacitors. *Microporous and Mesoporous Materials* 2019; **276**, 280-291.

[24] B Wang, J Qiu, H Feng, E Sakai and T Komiyama. KOH-activated nitrogen doped porous carbon nanowires with superior performance in supercapacitors. *Electrochimica Acta* 2016; **190**, 229-239.

[25] TM Dao and LL Tran. Synthesis of activated carbon from macadamia nutshells activated by H_2SO_4 and K_2CO_3 for methylene blue removal in water. *Bioresource Technology Reports* 2020; **12**, 100583.

[26] RJ Ramalingam, M Sivachidambaram, JJ Vijaya, HA Al-Lohedan and MR Muthumareeswaran. Synthesis of porous activated carbon powder formation from fruit peel and cow dung waste for modified electrode fabrication and application. *Biomass and Bioenergy* 2020; **142**, 105800.

[27] S Rovani, AG Rodrigues, LF Medeiros, R Cataluna, EC Lima and AN Fernandes. Synthesis and characterization of activated carbon from agroindustrial waste-preliminary study of 17β-estradiol removal from aqueous solution. *Journal of Environmental Chemical Engineering* 2016; **4(2)**, 2128-2137.

[28] A Kumar and HM Jena. Preparation and characterization of high surface area activated carbon from Fox nut (*Euryale ferox*) shell by chemical activation with H_3PO_4. *Results in Physics* 2016; **6**, 651-658.

[29] E Santoso, R Ediati, Y Kusumawati, H Bahruji, DO Sulistiono and D Prasetyoko. Review on recent advances of carbon-based adsorbent for methylene blue removal from wastewater. *Materials Today Chemistry* 2020; **16**, 100233.

[30] MJ Ahmed and SK Theydan. Microporous activated carbon from Siris seed pods by microwave-induced KOH activation for metronidazole adsorption. *Journal of Analytical and Applied Pyrolysis* 2013; **99**, 101-109.

[31] Y Luo, J Street, P Steele, E Entsminger and V Guda. Activated carbon derived from pyrolyzed pinewood char using elevated temperature, KOH, H_3PO_4, and H_2O_2. *BioResources* 2016; **11(4)**, 10433-10447.

[32] M Blachnio, A Derylo-Marczewska, B Charmas, M Zienkiewicz-Strzalka, V Bogatyrov and M Galaburda. Activated carbon from agricultural wastes for adsorption of organic pollutants. *Molecules* 2020; **25(21)**, 5105.

[33] LKCD Souza, JC Martins, DP Oliveira, CS Ferreira, AAS Gonçalves, RO Araujo, JDS Chaar, MJF Costa, DV Sampaio, RR Passos and LA Pocrifka. Hierarchical porous carbon derived from acai seed biowaste for supercapacitor electrode materials. *Journal of Materials Science: Materials in Electronics* 2020; **31**, 12148-12157.

[34] Y Elmaguana, N Elhadiri, M Bouchdoug, M Benchanaa and A Jaouad. Optimization of preparation conditions of activated carbon from walnut cake using response surface methodology. *Moroccan Journal of Chemistry* 2018; **6**, 92-105.

[35] M Thommes, K Kaneko, AV Neimark, JP Olivier, F Rodriguez-Reinoso, J Rouquerol and KSW Sing. Physisorption of gases, with special reference to the evaluation of surface area and pore size distribution (IUPAC Technical Report). *Pure and Applied Chemistry* 2015; **87(9-10)**, 1051-1069.

[36] AI Osman, J Blewitt, JK Abu-Dahrieh, C Farrell, AH Al-Muhtaseb, J Harrison and DW Rooney. Production and characterization of activated carbon and carbon nanotubes from potato peel waste and their application in heavy metal removal. *Environmental Science and Pollution Research* 2019; **26**, 37228-37241.

[37] MS Shamsuddin, NRN Yusoff and MA Sulaiman. Synthesis and characterization of activated carbon produced from kenaf core fiber using H_3PO_4

activation. *Procedia Chemistry* 2016; **19(9)**, 558-565.

[38] D Bergna, T Varila, H Romar and U Lassi. Comparison of the properties of activated carbons produced in one-stage and two-stage processes. *Journal of Carbon Research* 2018; **4(3)**, 41.

[39] KY Foo and BH Hameed. Preparation of activated carbon from date stones by microwave-induced chemical activation: Application for methylene blue adsorption. *Chemical Engineering Journal* 2011; **170(1)**, 338-344.

[40] HR Pouretedal and N Sadegh. Effective removal of amoxicillin, cephalexin, tetracycline and penicillin G from aqueous solutions using activated carbon nanoparticles prepared from vine wood. *Journal of Water Process Engineering* 2014; **1**, 64-73.

[41] H Boulika, ME Hajam, MH Nabih, NI Kandria and A Zerouale. Activated carbon from almond shells using an eco-compatible method: Screening, optimization characterization, and adsorption performance testing. *RSC Advances* 2022; **12(53)**, 34393-34403.

[42] NS Abdullah, MH Hussin, S Sharifuddin and MAM Yusoff. Preparation and characterization of activated carbon from Moringa oleifera seed pod. *Science International* 2017; **29(1)**, 7-11.

[43] PJ Osvaldo, LC Andre, CG Ralph, OB Erica, IPAF Souza, AC Martins, T Asefa and VC Almeida. Synthesis of $ZnCl_2$ activated carbon from macadamia nut endocarp (Macadamia integrifolia) by microwave-assisted pyrolysis: Optimization using RSM and methylene blue adsorption. *Journal of Analytical and Applied Pyrolysis* 2014; **105**, 166-176.

[44] WM El-Sayed, MH El-Kalyoubi, MM Mostafa and SA Farghal. Nutritional evaluation of roselle (*Hibiscus sabdariffa* L.) and its application in biscuit supplementation. *Arab Universities Journal of Agricultural Sciences* 2019; **27(5)**, 2563-2572.

[45] SO Salami and AJ Afolayan. Evaluation of nutritional and elemental compositions of green and red cultivars of roselle: *Hibiscus sabdariffa* L. *Scientific Reports* 2021; **11**, 1030.

[46] S Phewphong, W Roschat, K Namwongsa, A Wonam, T Kaisri, P Duangpakdee, T Leelatam, P Moonsin and V Promarak. Evaluation of the nutritional, minerals, and antioxidant potential of roselle (*Hibiscus sabdariffa* Linn.) seeds from Roi Et Province in the Northeastern Region of Thailand. *Trends in Sciences* 2023; **20(6)**, 6664.